

Large Amplitude Free Vibration Analysis of Thin Rectangular Plates: Simple Closed-form Solutions

Jagadish Babu Gunda¹

¹ Advanced Systems Laboratory, Kanchanbagh, Hyderabad 500058, India

Abstract. Large amplitude free vibration behavior of thin, isotropic rectangular plate configurations are expressed in the form of simple closed-form solutions by using an application of the Ritz method based on coupled displacement fields. Influence of plate aspect ratio ($\frac{a}{b}$) and Poisson ratio (ν) on the behavior of back-bone curves is briefly discussed for various boundary configurations of the rectangular plate. Proposed closed-form solutions are corrected for the simple harmonic motion (SHM) assumption using the well established harmonic balance method which is applicable for the homogeneous form of cubic non-linear Duffing equation.

Keywords. Large amplitude free vibration, Thin rectangular plates, Ritz method, Closed-form solutions, Coupled displacement fields, von-Kármán type of geometric non-linearity, Non-linear frequency.

Nomenclature

a = length of the rectangular plate
 b = width of the rectangular plate
 C = axial rigidity of the plate $\left(\frac{Eh}{(1-\nu^2)}\right)$
 D = flexural rigidity of the plate $\left(\frac{Eh^3}{12(1-\nu^2)}\right)$
 E = Young's modulus
 h = thickness of the plate
 N_x, N_y and N_{xy} = in-plane stress resultants
 M_x, M_y and M_{xy} = moment resultants
 u = displacement in x -direction
 v = displacement in y -direction
 U = strain energy of the plate
 w = transverse displacement

T = kinetic energy of the plate

x, y = in-plane co-ordinates

z_1 = maximum reference amplitude of the rectangular plate

$\frac{z_1}{h}$ = maximum reference amplitude to thickness ratio

ϵ_x, ϵ_y and ϵ_{xy} = in-plane strain terms

λ_L = linear frequency parameter $\left(\frac{\rho h \omega_L^2 a^4}{\pi^4 D}\right)$

λ_{NLH} = non-linear frequency parameter obtained on the basis of SHM assumption $\left(\frac{\rho h \omega_{NLH}^2 a^4}{\pi^4 D}\right)$

λ_{NL} = non-linear frequency parameter $\left(\frac{\rho h \omega_{NL}^2 a^4}{\pi^4 D}\right)$

ν = Poisson ratio

ψ_x, ψ_y and ψ_{xy} = curvature terms

Subscripts

L = linear

NL = non-linear

NLH = non-linear based on harmonic motion assumption

x = partial derivative with respect to x

xx = second partial derivative with respect to x

y = partial derivative with respect to y

yy = second partial derivative with respect to y

xy = partial derivative with respect to x and y

1 Introduction

Large amplitude free vibration behavior of plates [1–18] have received considerable attention by various researchers due to its relative importance to the field of structural engineering. Leung and Mao [7] applied an Hamilton's formulation and symplectic integration methods to investigate the non-linear vibration behavior of beams and plates. Amabili and Carra [10] investigated the experimental large amplitude forced vibration behavior of thin rectangular plate carrying different concentrated masses. Recently, Gunda [11, 12] simplified the problem of thermal post-buckling and large amplitude free vibration behavior of various square plate configurations resting on elastic foundation in the form of simple closed-form solutions by using an application of coupled displacement fields (CDF) in the Rayleigh-Ritz method. Leissa [13] discussed the historical basis of Rayleigh and Ritz methods and concluded that the

Corresponding author: Jagadish Babu Gunda, E-mail: jagadishasl@gmail.com.

Received: 30 November 2012. Accepted: 13 April 2013.

Rayleigh's name should not be attached to the Ritz method. Comprehensive literature review pertaining to the large amplitude free vibration behavior of plates is already discussed by the author in the Ref. [11] and not much attention is focused here on the same.

The main objective of the proposed work is to revisit the applicability of the study proposed and assumptions stated in the Ref. [11] for evaluating the large amplitude free vibration behavior of thin, isotropic rectangular plate configurations. Numerical accuracy of the proposed closed-form solutions related to the rectangular plates are compared with the available literature values which indicates the versatile nature of the formulation discussed in Ref. [11]. Influence of plate aspect ratio ($\frac{a}{b}$) and Poisson ratio (ν) on large amplitude free vibration behavior of various thin rectangular plate configurations is briefly discussed.

2 Large Amplitude Free Vibration Analysis of Thin Rectangular Plates: Simple Closed-form Solutions

Fig. 1 shows a typical thin rectangular plate, where the in-plane displacements of the plate are assumed to be constrained which induces the von-Kármán type of geometric non-linearity due to the membrane stretching action of the plate. Following assumptions are used for the analysis of thin rectangular plates considered in this study:

- Material of the plate is elastic, homogeneous, and isotropic.
- The straight lines, initially normal to the plate median surface before deformation, remain straight and normal to the middle surface during the deformation, and the length of such elements is not altered.
- Shearing forces, N_{xy} and N_{yx} are assumed to vanish or N_{xy} and N_{yx} may remain as constant.
- Edges at $x=0$ and $x=a$ are free to move in the y -direction and edges at $y=0$ and $y=b$ are free to move in the x -direction.

The third assumption stated here is slightly different with reference to the assumption stated in the author's previous works [11, 12] which deals with the analysis of square plates where the membrane stretching forces are assumed to be uniform on either side of the square plate and subsequently it is assumed that it results in the absence of shearing forces. In case of a rectangular plate, it is assumed that the net resultant stretching forces (N_x and N_y) may not be equal in magnitude on either side of the plate and the net resultant shearing forces (N_{xy} and N_{yx}) are assumed to remain as constant. However, the formulation discussed in Ref. [11] remains unaffected with the above stated assumption and directly it can be applied for the analysis of rectangular plates.

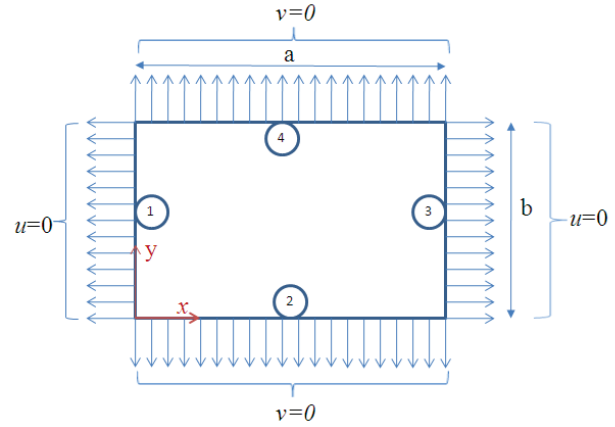


Figure 1. A rectangular plate subjected to in-plane forces (In-plane displacements are constrained to move as shown in this figure).

The strain-displacement relations of a plate mid-plane considering the von-Kármán type of geometric non-linearity are expressed as follows

$$\epsilon_x = u_x + \frac{1}{2}w_x^2 \quad (1)$$

$$\epsilon_y = u_y + \frac{1}{2}w_y^2 \quad (2)$$

$$\epsilon_{xy} = u_y + v_x + w_x w_y \quad (3)$$

$$\psi_x = -w_{xx} \quad (4)$$

$$\psi_y = -w_{yy} \quad (5)$$

$$\psi_{xy} = -2w_{xy} \quad (6)$$

Strain energy of a thin rectangular plate can be expressed in terms of its in-plane strains and curvature terms as follows

$$U = \frac{1}{2} \int_0^b \int_0^a C \left[\epsilon_x^2 + \epsilon_y^2 + 2\nu\epsilon_x\epsilon_y + \frac{(1-\nu)}{2}\epsilon_{xy}^2 \right] + D \left[\psi_x^2 + \psi_y^2 + 2\nu\psi_x\psi_y + \frac{(1-\nu)}{2}\psi_{xy}^2 \right] dx dy \quad (7)$$

The kinetic energy of the rectangular plate, neglecting in-plane inertia, with the assumption of SHM can be expressed as follows

$$T = \frac{1}{2}\rho h \int_0^b \int_0^a \dot{w}^2 dx dy = \frac{\omega^2}{2}\rho h \int_0^b \int_0^a w^2 dx dy \quad (8)$$

Where \dot{w} denotes the first derivative of w with reference to time.

Table 1. Approximate lateral displacement field ($w(x, y)$) variations assumed in Ritz method for various rectangular plate configurations (H-Hinged, C-Clamped, G-Guided).

Boundary Configuration	w
HHHH	$z_1 \sin\left(\frac{\pi x}{a}\right) \sin\left(\frac{\pi y}{b}\right)$
CCCC	$\frac{z_1}{4} (1 - \cos(2\frac{\pi x}{a})) (1 - \cos(2\frac{\pi y}{b}))$
CHCH	$\frac{z_1}{2} (1 - \cos(2\frac{\pi x}{a})) \sin\left(\frac{\pi y}{b}\right)$
HHGG	$z_1 \cos\left(\frac{\pi x}{2a}\right) \cos\left(\frac{\pi y}{2b}\right)$
CCGG	$\frac{z_1}{4} (1 - \cos(\frac{\pi x}{a})) (1 - \cos(\frac{\pi y}{b}))$

The total potential energy of the rectangular plate can be expressed as follows

$$\Pi = U - T \quad (9)$$

Following author's previous work [11] considering the above stated assumptions, the in-plane displacement field (u) can be simply expressed as follows:

$$u = - \int \left(\int (w_x w_{xx} - v w_y w_{xy}) dx \right) dx + C_1 x + C_2 \quad (10)$$

Where C_1 and C_2 are constants of integration and these constants can be obtained by using the immovable in-plane edge boundary conditions ($u(0, y) = 0$ and $u(a, y) = 0$) along the x -direction of the plate.

Similarly, following the author's previous work [11], the in-plane displacement field (v) can be simply expressed as follows:

$$v = - \int \left(\int (w_y w_{yy} - v w_x w_{xy}) dy \right) dy + C_3 y + C_4 \quad (11)$$

Where C_3 and C_4 are constants of integration and these constants can be obtained by using the immovable in-plane edge boundary conditions ($v(x, 0) = 0$ and $v(x, b) = 0$) along the y -direction of the plate.

Assumed approximate lateral displacement field variations for various rectangular plate configurations are shown in Table. 1 (which satisfy the essential boundary conditions shown in Table 2). Eqs. (10) and (11) are used to derive an approximate in-plane displacement field variations of the plate, where the immovable in-plane edge boundary conditions of the plate are discussed in Table 2. In-plane displacement field variations obtained by using Eqs. (10) and (11) are shown in Tables 3 and 4.

These assumed (w) (Table 1) and derived displacement field variations (u and v) (Tables 3 and 4) obtained by using Eqs. (10) and (11) are substituted in the strain energy (U) and the kinetic energy (T) expressions. Minimization of the total potential energy ($\frac{\partial \Pi}{\partial z_1} = 0$) (Eq. (9)) ex-

pression with reference to the unknown displacement field co-efficient (z_1) results in linear frequency parameter when linear strain displacement relations are used for each boundary configuration. The use of non-linear strain displacement relations in the process of minimization of total potential energy (Π) results in arriving at simple closed-form expressions for the non-linear frequency (ω_{NLH}) of the rectangular plate based on the SHM assumption. The non-dimensional parameters obtained corresponding to the linear and the non-linear frequency parameters of various rectangular plate configurations are shown in Tables 5 and 6. Observation of the closed-form solutions presented in Table 6 indicates that the plate exhibits conventional cubic nonlinearity which is governed by the homogeneous form of Duffing equation. Frequency parameters (λ_{NLH}) presented in Table 6 are obtained on the basis of SHM assumption and these expressions can be corrected by using the harmonic balance method (HBM) discussed in Refs. [16, 17]. The non-linear frequency parameters (λ_{NL}) which are obtained after correcting for the SHM assumption using the HBM method discussed in Refs. [16, 17] are indicated in Table 7. For the sake of brevity, the HBM method is not discussed here and readers can refer to these Refs. [16–18] for more details on HBM.

3 Results and Discussion

Numerical accuracy of the closed-form solutions presented in Tables 5, 6 and 7 by using the Ritz method based on coupled displacement fields approach are compared to the available literature values in Tables 8 and 9 for various aspect ratio ($\frac{a}{b} = 1.0$ and 2.0) of the plate. Poisson's ratio is considered as 0.3 for all the numerical calculations shown in this study. It can be observed that the numerical results presented in Tables 8 and 9 by using the Ritz method based on CDF approach shows good comparison with available literature values for the non-linear to linear frequency ratios ($\frac{\omega_{NLH}}{\omega_L}$ or $\frac{\omega_{NL}}{\omega_L}$) obtained with or without the assumption of SHM. For few boundary configurations numerical results are not readily available for comparison purpose and for these configurations numerical results are presented for future reference. Linear frequency parameters obtained from the commercially available finite element software (ANSYS) [19, 20] are compared with the present results for all the boundary configurations. Figs. 2-3 shows the influence of plate aspect ratio ($\frac{a}{b}$) on the behavior of back-bone curves of various rectangular plate configurations for $\nu=0.3$. In general, it is observed that non-linear to linear frequency ratio ($\frac{\omega_{NL}}{\omega_L}$) increases with an increase in plate aspect ratio of the plate for any given maximum reference amplitude of the plate. Finally, influence of Poisson ratio (ν) on variation in frequency ratio ($\frac{\omega_{NL}}{\omega_L}$) is shown in Fig. 4 for various plate configuration which indicates that

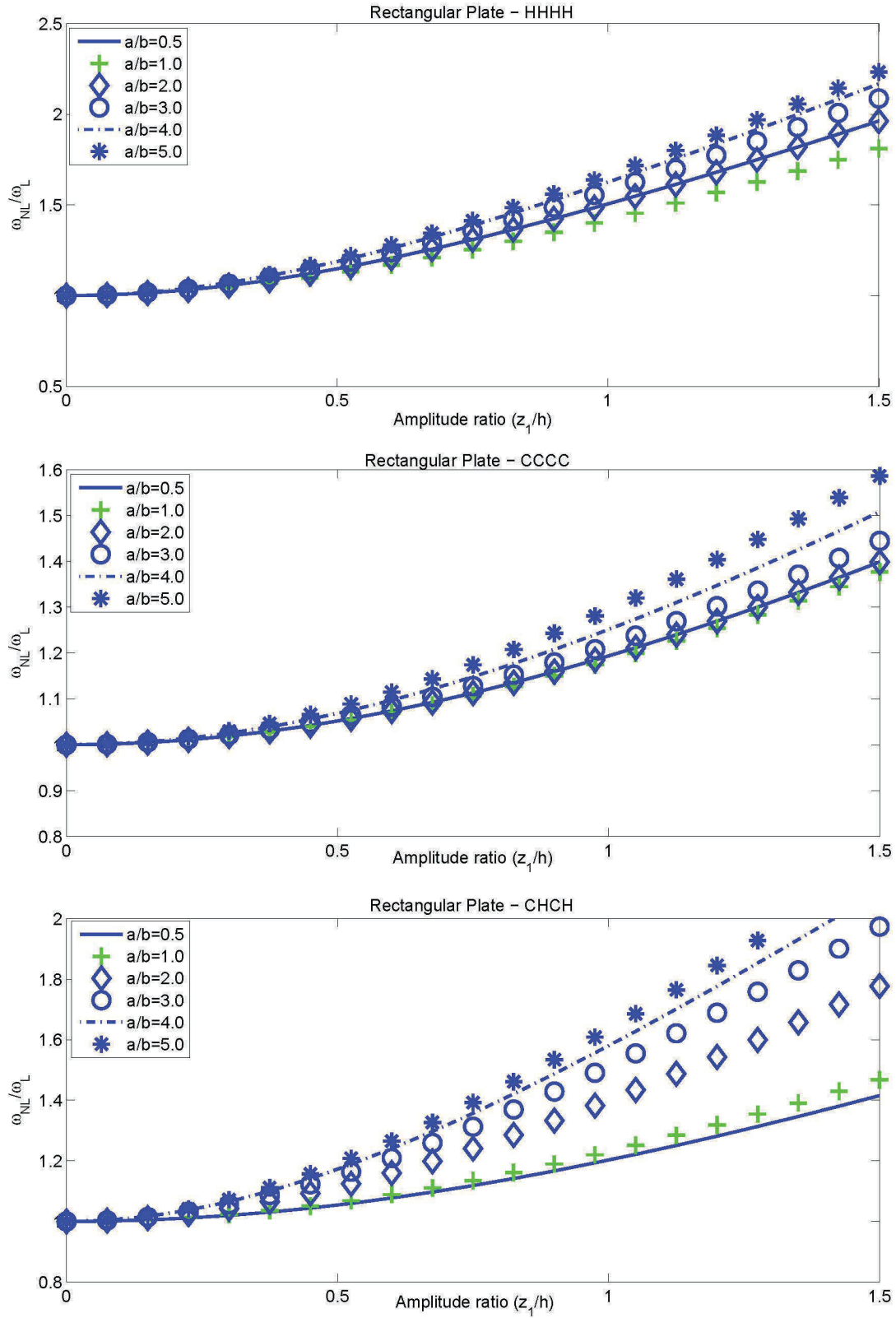


Figure 2. Back-bone curves indicates the influence of aspect ratio (a/b) of various rectangular plates obtained by using the proposed closed-form solutions for $\nu=0.3$

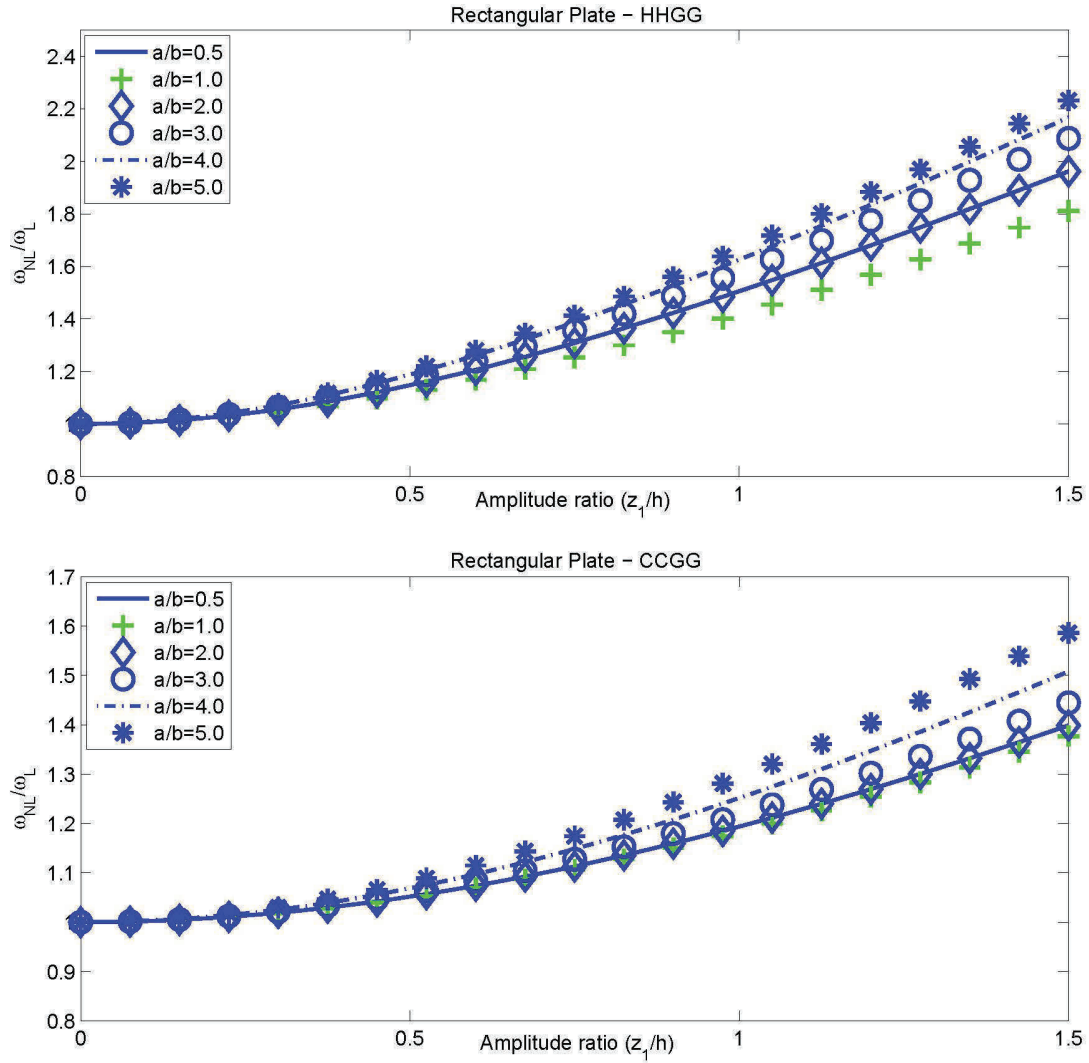


Figure 3. Back-bone curves indicates the influence of aspect ratio (a/b) of various rectangular plates obtained by using the proposed closed-form solutions for $\nu=0.3$

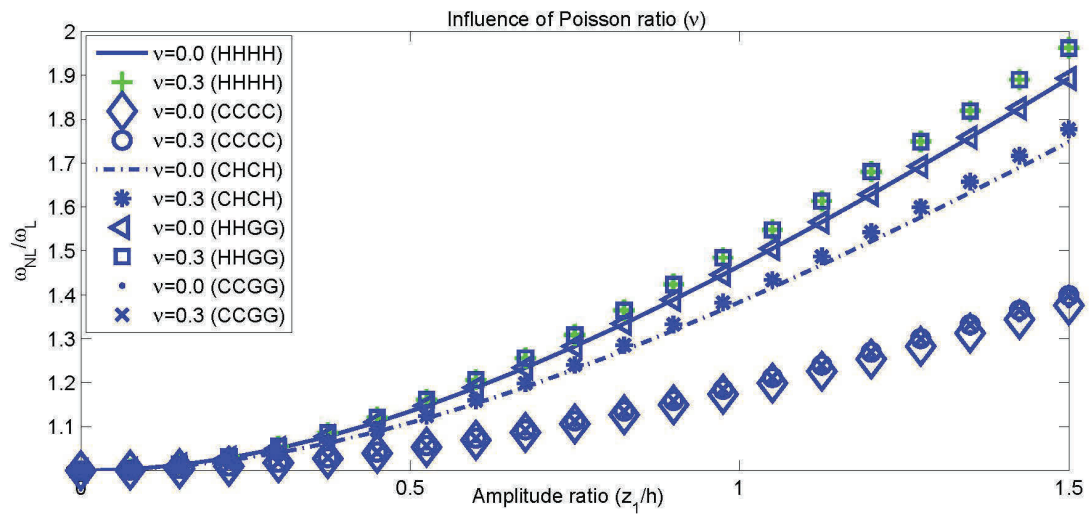


Figure 4. Influence of Poisson ratio (ν) on variation of Back-bone curves of various rectangular plate configurations ($a/b=2$)

Table 2. Essential edge boundary conditions considered for the various rectangular plate configurations with the additional in-plane displacement constraints ($u(0, y)=u(a, y)=v(x, 0)=v(x, b)=0$).

S.No.	Plate configuration	Boundary conditions on w
1	HHHH	$w(0, y) = w(x, 0) = w(a, y) = w(x, b) = 0$
2	CCCC	$w(0, y) = w(x, 0) = w(a, y) = w(x, b) = 0$ $w'(0, y) = w'(x, 0) = w'(a, y) = w'(x, b) = 0$
3	CHCH	$w(0, y) = w(x, 0) = w(a, y) = w(x, b) = 0$ $w'(0, y) = w'(a, y) = 0$
4	HHGG	$w(0, y) = w(x, 0) = w'(a, y) = w'(x, b) = 0$
5	CCGG	$w(0, y) = w(x, 0) = w'(0, y) = w'(x, 0)$ $w'(a, y) = w'(x, b) = 0$

in general an increase in Poisson ratio (ν) results in an increase in frequency ratio for any given maximum reference amplitude of the plate.

4 Conclusions

Large amplitude free vibration behavior of thin, isotropic rectangular plates are expressed in the form of simple closed-form solutions by using the Ritz method based on CDF approach. Geometric non-linearity of von-Kármán type is taken into consideration which accounts for membrane stretching action of the rectangular plate. Numerical accuracy of the proposed closed-form solutions obtained from the Ritz method are compared to the available literature results which indicates the wider applicability of the formulation discussed in the Ref. [11].

References

- [1] S. Goswami, T. Kant, Large amplitude vibration of polymer composite stiffened laminates by the finite element method, *J. Reinforc. Plast. and Comp.* 18(5), 421-436 (1999).
- [2] W. Han, M. Petyt, Geometrically nonlinear vibration analysis of thin, rectangular plates using the hierarchical finite element method-I: The fundamental mode of isotropic plates, *Comp. Struct.* 63(2), 295-308 (1997).
- [3] A.K. Dash, Large amplitude free vibration analysis of composite plates by finite element method, M.Tech thesis, National Institute of Technology, Rourkela, May 2010.
- [4] L. Azrar, R. Benamar, M. Potier-Ferry, An Asymptotic-numerical method for large amplitude free vibrations of thin elastic plates, *J. Sou. Vib.* 220(4), 695-727 (1999).
- [5] S.L. Lau, Y.K. Cheung, S.Y. Wu, Nonlinear vibration of thin elastic plates Part I: Generalized incremental Hamilton's principle and finite element formulation, *J. App. Mech.* 51, 837-844 (1984).
- [6] N. Yamaki, Influence of large amplitudes on flexural vibrations of elastic plates, *Z. Angew. Math. Mech. (ZAMM)*, 41 (12), 501-510 (1961).
- [7] A.Y.T. Leung, S.G. Mao, A symplectic Galerkin method for non-linear vibration of beams and plates. *J. Sou. & Vib.* 183(3), 475-491 (1995).
- [8] S.L.Lau, Incremental harmonic balance method for nonlinear structural vibrations. Ph.D Thesis, University of Hong Kong (1982).
- [9] G.V. Rao, I.S. Raju, K.K. Raju, A finite element formulation for large amplitude flexural vibrations of thin rectangular plates, *Comp. & Struct.* 6, 163-167 (1976).
- [10] M. Amabili, S. Carra, Experiments and simulations for large-amplitude vibrations of rectangular plates carrying concentrated masses. *J. Sou. & Vib.* 331, 155-166 (2012).
- [11] J.B.Gunda, Large amplitude free vibration analysis of square plates resting on elastic foundation: A simple closed-form solutions, *Z. Angew. Math. Mech. (ZAMM)*, 1-12 (2012) / DOI 10.1002/zamm.201200126.
- [12] J.B.Gunda, Thermal post-buckling analysis of square plates resting on elastic foundation: A simple closed-form solutions, *App. Math. Model.* 37, 5536-5548 (2013).
- [13] A.W.Leissa, The historical bases of the Rayleigh and Ritz methods. *J. Sou. & Vib.* 287, 961-978 (2005).
- [14] M. Amabili, Nonlinear vibrations of rectangular plates with different boundary conditions: theory and experiments, *Computers and Structures* 82 (2004) 2587-2605.
- [15] M. Taazount, A. Zinai, A. Bouazzouni, Large free vibration of thin plates: Hierarchic finite Element Method and asymptotic linearization. *Euro. J. of Mechs. of Sol.* 28, 155-165 (2009).
- [16] R.K. Gupta, J.B. Gunda, G. Ranga Janardhan, G. Venkateswara Rao, Relatively simple finite element formulation for the large amplitude free vibrations of uniform beams, *Finite Elements in Anal. and Des.* 45 (10), 624-631 (2009).
- [17] J.B. Gunda, R.K. Gupta, G. Ranga Janardhan, G. Venkateswara Rao, Large amplitude free vibration analysis of Timoshenko beams using a relatively simple finite element formulation, *Int. J. Mech. Sci.*, 52(12), 1597-1604 (2010).
- [18] J.B. Gunda, R.K. Gupta, G. Ranga Janardhan, G. Venkateswara Rao, Large amplitude vibration analysis of composite beams: Simple closed-form solutions, *Composite Structures* 93(2), 870-879 (2011).
- [19] ANSYS Inc. , ANSYS package version 10.0 , Canonsburgh PA, USA.
- [20] ANSYS, Inc. Theory Reference.

Table 3. In-plane displacement field variations $u(x, y)$ for various rectangular plates obtained by using Eq. (10)

Boundary configuration	In-plane displacement field variation $u(x, y)$
HHHH	$-\frac{z_1^2 \pi}{4a^2 b^2} (b^2 a \sin(\frac{\pi x}{a}) \cos(\frac{\pi x}{a}) - b^2 a \sin(\frac{\pi x}{a}) \cos(\frac{\pi y}{b}))^2 - \nu (\cos(\frac{\pi y}{b}))^2 a^3 \sin(\frac{\pi x}{a}) \cos(\frac{\pi x}{a})$
CCCC	$-\frac{z_1^2 \pi}{32ab^2} (-b^2 \sin(2\frac{\pi x}{a}) \cos(2\frac{\pi x}{a}) + 2b^2 \cos(2\frac{\pi x}{a}) \sin(2\frac{\pi y}{b}) \sin(2\frac{\pi x}{a}) - b^2 (\cos(2\frac{\pi y}{b}))^2 \sin(2\frac{\pi x}{a}) \cos(2\frac{\pi x}{a})$ $-4\nu a^2 \sin(2\frac{\pi x}{a}) + 4\nu a^2 \sin(2\frac{\pi x}{a}) (\cos(2\frac{\pi y}{b}))^2 + \nu a^2 \sin(2\frac{\pi x}{a}) \cos(2\frac{\pi x}{a}) \cos(2\frac{\pi y}{b}) (\cos(2\frac{\pi y}{b}))^2$
CHCH	$\frac{z_1^2 \pi}{32a^2 b^2} (4b^2 \sin(2\frac{\pi x}{a}) \cos(2\frac{\pi x}{a}) a - 4b^2 \sin(2\frac{\pi x}{a}) \cos(2\frac{\pi x}{a}) a (\cos(\frac{\pi y}{b}))^2 + 4\nu (\cos(\frac{\pi y}{b}))^2 a^3 \sin(2\frac{\pi x}{a}) \cos(2\frac{\pi x}{a})$ $-2 (\cos(1/2\frac{\pi y}{b}))^2 b^2 \cos(1/2\frac{\pi x}{a}) \sin(1/2\frac{\pi x}{a}) + 2\nu a^2 \cos(1/2\frac{\pi x}{a}) \sin(1/2\frac{\pi x}{a}) \sin(1/2\frac{\pi y}{b}) (\cos(1/2\frac{\pi y}{b}))^2$
HHGG	$-\frac{z_1^2 \pi}{16b^2 a} (-b^2 \sin(\frac{\pi x}{a}) \cos(\frac{\pi x}{a}) + 2b^2 \cos(\frac{\pi x}{a}) \sin(\frac{\pi x}{a}))^2 \sin(\frac{\pi y}{b}) \cos(\frac{\pi x}{a}) - 2\nu a^2 \cos(1/2\frac{\pi x}{a}) \sin(1/2\frac{\pi x}{a}) (\cos(1/2\frac{\pi y}{b}))^2$
CCGG	$-\frac{z_1^2 \pi}{64ab^2} (-b^2 \sin(\frac{\pi x}{a}) \cos(\frac{\pi x}{a}) + 2b^2 \cos(\frac{\pi x}{a}) \sin(\frac{\pi x}{a}))^2 \sin(\frac{\pi y}{b}) \cos(\frac{\pi x}{a}) - 4\nu a^2 \sin(\frac{\pi x}{a})$ $+4\nu a^2 \sin(\frac{\pi x}{a}) (\cos(\frac{\pi y}{b}))^2 + \nu a^2 \sin(\frac{\pi x}{a}) \cos(\frac{\pi x}{a}) (\cos(\frac{\pi y}{b}))^2$

Table 4. In-plane displacement field variations $v(x, y)$ for various rectangular plates obtained by using Eq. (11)

Boundary configuration	In-plane displacement field variation $u(x, y)$
HHHH	$-\frac{z_1^2 \pi}{4a^2 b^2} (a^2 b \sin(\frac{\pi y}{b}) \cos(\frac{\pi y}{b}) - a^2 b \sin(\frac{\pi y}{b}) \cos(\frac{\pi x}{a}))^2 - \nu (\cos(\frac{\pi x}{a}))^2 b^3 \sin(\frac{\pi y}{b}) \cos(\frac{\pi y}{b})$
CCCC	$-\frac{z_1^2 \pi}{32a^2 b} (-a^2 \sin(2\frac{\pi y}{b}) \cos(2\frac{\pi y}{b}) + 2a^2 \cos(2\frac{\pi y}{b}) \sin(2\frac{\pi x}{a}) \sin(2\frac{\pi y}{b}) - a^2 (\cos(2\frac{\pi x}{a}))^2 \sin(2\frac{\pi y}{b}) \cos(2\frac{\pi y}{b})$ $-4\nu b^2 \sin(2\frac{\pi y}{b}) + 4\nu b^2 \sin(2\frac{\pi y}{b}) (\cos(2\frac{\pi x}{a}))^2 + \nu b^2 \sin(2\frac{\pi y}{b}) \cos(2\frac{\pi y}{b}) \cos(2\frac{\pi x}{a}) (\cos(2\frac{\pi x}{a}))^2$
CHCH	$\frac{z_1^2 \pi}{32a^2 b^2} (4b^2 \sin(2\frac{\pi x}{a}) \cos(2\frac{\pi x}{a}) a - 4b^2 \sin(2\frac{\pi x}{a}) \cos(2\frac{\pi x}{a}) a (\cos(\frac{\pi y}{b}))^2 + 4\nu (\cos(\frac{\pi y}{b}))^2 a^3 \sin(2\frac{\pi x}{a}) \cos(2\frac{\pi x}{a})$ $-2 (\cos(1/2\frac{\pi x}{a}))^2 a^2 \cos(1/2\frac{\pi y}{b}) \sin(1/2\frac{\pi y}{b}) + 2\nu b^2 \cos(1/2\frac{\pi y}{b}) \sin(1/2\frac{\pi y}{b}) - 2\nu b^2 \cos(1/2\frac{\pi y}{b}) \sin(1/2\frac{\pi x}{a}) (\cos(1/2\frac{\pi x}{a}))^2$
HHGG	$-\frac{z_1^2 \pi}{16a^2 b} (-a^2 \sin(\frac{\pi y}{b}) \cos(\frac{\pi y}{b}) + 2a^2 \cos(\frac{\pi y}{b}) \sin(\frac{\pi x}{a}) \sin(\frac{\pi y}{b}) - a^2 (\cos(\frac{\pi x}{a}))^2 \sin(\frac{\pi y}{b}) \cos(\frac{\pi y}{b})$ $-4\nu b^2 \sin(\frac{\pi y}{b}) (\cos(\frac{\pi x}{a}))^2 + \nu b^2 \sin(\frac{\pi y}{b}) \cos(\frac{\pi y}{b}) - \nu b^2 \sin(\frac{\pi y}{b}) \cos(\frac{\pi x}{a}) (\cos(\frac{\pi x}{a}))^2$

Table 5. Non-dimensional linear (λ_L) frequency parameters of rectangular plates with various end boundary conditions obtained by using the Ritz method

	λ_L
HHHH	$\frac{a^4+b^4+2a^2b^2}{b^4}$
CCCC	$\frac{16}{9} \frac{3b^4+2b^2a^2+3a^4}{b^4}$
CHCH	$\frac{1}{3} \frac{8a^2b^2+3a^4+16b^4}{b^4}$
HHGG	$\frac{1}{16} \frac{a^4+2b^2a^2+b^4}{b^4}$
CCGG	$\frac{1}{9} \frac{3b^4+2b^2a^2+3a^4}{b^4}$

Table 6. Non-linear ($\frac{\lambda_{NLH}}{\lambda_L}$) frequency parameters of various rectangular plates with various end boundary conditions obtained by using the Ritz method

	$\frac{\lambda_{NLH}}{\lambda_L}$
HHHH	$1 + \left(\frac{-1}{16} \frac{3v^3a^8-6v^3a^4b^4+3v^3b^8-3v^2b^8+6v^2a^2b^6+6v^2a^2b^6-3v^2a^8-6v^2a^4b^4-48va^4b^4-36a^6b^2-36a^2b^6}{(a^2+b^2)^2b^2a^2} \right) \left(\frac{z_1}{h} \right)^2$
CCCC	$1 + \left(\frac{-1}{256} \frac{-6v^3a^4b^4+195b^8v^3+195a^8v^3+6a^6v^2b^2-195b^8v^2+6v^2a^2b^6-195a^8v^2-6v^2a^4b^4+96a^6v^2b^2-420a^2b^6-216va^4b^4}{a^2b^2(2a^2b^2+3a^4+3b^4)} \right) \left(\frac{z_1}{h} \right)^2$
CHCH	$1 + \left(\frac{-1}{256} \frac{195a^8v^3-96v^3a^4b^4+768b^8v^3+384v^2a^2b^6-195a^8v^2-768b^8v^2-3b^8v^2-3b^8v^2+6v^2b^6a^2-3b^8v^2-6v^2b^4a^4+6v^2b^6a^2-3b^8v^2-3b^8v^2+6a^6v^2b^2-6v^2b^4a^4-48va^4b^4-36a^6b^2-36a^2b^6}{a^2b^2(8a^2b^2+3a^4+16b^4)} \right) \left(\frac{z_1}{h} \right)^2$
HHGG	$1 + \left(\frac{-1}{16} \frac{3a^8v^3+3b^8v^3-6v^3b^4a^4+6v^2b^6a^2-3b^8v^2-3b^8v^2+6a^6v^2b^2-6v^2b^4a^4-48va^4b^4-36a^6b^2-36a^2b^6}{(b^2+a^2)^2b^2a^2} \right) \left(\frac{z_1}{h} \right)^2$
CCGG	$1 + \left(\frac{-1}{256} \frac{195a^8v^3-6v^3a^4b^4+195b^8v^3-195b^8v^2+6a^6b^2v^2-195a^8v^2+6v^2a^4b^4+96a^6v^2b^2-216va^4b^4-420a^2b^6-216a^6b^2-216a^4b^4}{a^2b^2(3a^4+2a^2b^2+3b^4)} \right) \left(\frac{z_1}{h} \right)^2$

Table 7. Non-linear ($\frac{\lambda_{NL}}{\lambda_L}$) frequency parameters of various rectangular plates after correction for SHM assumption using the harmonic balance method discussed in Refs. [16, 17]

	$\frac{\lambda_{NL}}{\lambda_L}$
HHHH	$1 + \frac{3}{4} \left(\frac{-1}{16} \frac{3\nu^3 a^8 - 6\nu^3 a^4 b^4 + 3\nu^3 b^8 - 3\nu^2 b^8 + 6\nu^2 a^2 b^6 + 6\nu^2 a^6 b^2 - 3\nu^2 a^8 - 6\nu^2 a^4 b^4 - 48\nu a^4 b^4 - 36a^6 b^2 - 36a^2 b^6}{(a^2 + b^2)^2 b^2 a^2} \right) \left(\frac{z_1}{h} \right)^2$
CCCC	$1 + \frac{3}{4} \left(\frac{-1}{256} \frac{-6\nu^3 a^4 b^4 + 195b^8 \nu^3 + 195a^8 \nu^3 + 6a^6 \nu^2 b^2 - 195b^8 \nu^2 + 6\nu^2 a^2 b^6 - 195a^8 \nu^2 - 96\nu^3 a^4 b^4 + 768b^8 \nu^3 + 384\nu^2 a^2 b^6 - 195a^8 \nu^2 - 768b^8 \nu^2 + 24a^6 \nu^2 b^2 - 96\nu^2 a^4 b^4 + 96a^6 \nu b^2 + 96\nu a^2 b^6 - 420a^2 b^6 - 420a^6 b^2 - 216a^4 b^4}{a^2 b^2 (2a^2 b^2 + 3a^4 + 3b^4)} \right) \left(\frac{z_1}{h} \right)^2$
CHCH	$1 + \frac{3}{4} \left(\frac{-1}{256} \frac{195a^8 \nu^3 - 96\nu^3 a^4 b^4 + 768b^8 \nu^3 + 384\nu^2 a^2 b^6 - 195a^8 \nu^2 - 768b^8 \nu^2 - 3b^8 \nu^2 - 3a^8 \nu^2 + 6a^6 \nu^2 b^2 - 6\nu^2 b^4 a^4 - 48\nu b^4 a^4 - 36a^6 b^2 - 36b^6 a^2}{a^2 b^2 (8a^2 b^2 + 3a^4 + 16b^4)} \right) \left(\frac{z_1}{h} \right)^2$
HHGG	$1 + \frac{3}{4} \left(\frac{-1}{16} \frac{3a^8 \nu^3 + 3b^8 \nu^3 - 6\nu^3 b^4 a^4 + 6\nu^2 b^6 a^2 - 3b^8 \nu^2 - 3a^8 \nu^2 + 6a^6 \nu^2 b^2 - 6\nu^2 b^4 a^4 - 48\nu b^4 a^4 - 36a^6 b^2 - 36b^6 a^2}{(b^2 + a^2)^2 b^2 a^2} \right) \left(\frac{z_1}{h} \right)^2$
CCGG	$1 + \frac{3}{4} \left(\frac{-1}{256} \frac{195a^8 \nu^3 - 6\nu^3 a^4 b^4 + 195b^8 \nu^3 - 195b^8 \nu^2 + 6a^6 b^2 \nu^2 - 195a^8 \nu^2 + 6\nu^2 a^2 b^6 - 6\nu^2 b^4 a^4 + 96a^6 \nu b^2 + 96\nu a^2 b^6 - 216\nu a^4 b^4 - 420a^2 b^6 - 420a^6 b^2 - 216a^4 b^4}{a^2 b^2 (3a^4 + 2a^2 b^2 + 3b^4)} \right) \left(\frac{z_1}{h} \right)^2$

Table 8. Comparison of non-linear ($\frac{\omega_{NLH}}{\omega_L}$) and linear (λ_L) frequency parameters of various rectangular plates obtained by using the Ritz method and the available literature results ($\nu=0.3$)

$\frac{z_1}{h}$	$\frac{a}{b}=1.0$					
	HHHH	CCCC	CHCH	HHGG	CCGG	
0.2	Present	Present	Present	Present	Present	
0.4	1.0266	1.0106	1.0136	1.0266	1.0106	
0.6	1.1027	1.0416	1.0533	1.1027	1.0416	
0.8	1.2190	1.2165	1.0894	1.1230	1.0914	
1	1.3653	1.3629	1.1521	1.2067	1.1575	
λ_L	4.0000	14.2220	1.2260	1.2978	1.5330	1.1575
			9.0000	0.2500	0.8889	
$\frac{z_1}{h}$	$\frac{a}{b}=2.0$					
	HHHH	CCCC	CHCH	HHGG	CCGG	
0.2	Present	Present	Present	Present	Present	
0.4	1.0332	1.0113	1.0252	1.0332	1.0113	
0.6	1.1270	1.0443	1.0975	1.1270	1.0443	
0.8	1.2680	1.0972	1.2084	1.2680	1.0972	
1	1.4424	1.1673	1.3484	1.4424	1.1673	
λ_L	25.0000	104.8889	32.0000	1.6396	1.2516	6.5556

Table 9. Comparison of non-linear ($\frac{\omega_{NL}}{\omega_L}$) and linear (λ_L) frequency parameters for various rectangular plates by using the Ritz method and the available literature results ($\nu=0.3$)

$\frac{a}{b}=1.0$												
$\frac{z_1}{h}$	HHHH				CCCC				CHCH		HHGG	
	Present	Ref. [4]	Ref. [5]	Ref. [6]	Present	Ref. [4]	Ref. [5]	Ref. [6]	Present	Ref. [6]	Present	Present
0.2	1.0200	1.0198	1.0196	1.0196	1.0079	1.0072	1.0073	1.0085	1.0102	1.0102	1.0200	1.0079
0.4	1.0780	1.0767	1.0763	1.0761	1.0314	1.0286	1.0291	1.0292	1.0402	1.0402	1.0780	1.0314
0.6	1.1681	1.1660	1.1645	1.1642	1.0693	1.0632	1.0648	1.0661	1.0885	1.0885	1.1681	1.0693
0.8	1.2837	1.2812	1.2779	1.2774	1.1202	1.1098	1.1138	1.1136	1.1526	1.1526	1.2837	1.1202
1	1.4186	1.4167	1.4109	1.4097	1.1825	1.1667	1.1762	1.1674	1.2301	1.2301	1.4186	1.1825
λ_L (Present)	4.0000				14.2220				9.0000	9.0000	0.2500	0.8889
λ_L (ANSYS)	3.9700				13.2650				8.5684	8.5684	0.2500	0.8304
$\frac{a}{b}=2.0$												
$\frac{z_1}{h}$	HHHH				CCCC				CHCH		HHGG	
	Present	Ref. [7]	Ref. [8]	Ref. [9]	Present	Ref. [9]			Present		Present	Present
0.2	1.0250	1.0241	1.0244	1.0239	1.0085	1.0073			1.0190	1.0190	1.0250	1.0085
0.4	1.0966	1.0927	1.0909	1.0918	1.0334	1.0292			1.0740	1.0740	1.0966	1.0334
0.6	1.2066	1.1975	1.1992	1.1957	1.0737	1.0647			1.1598	1.1598	1.2066	1.0738
0.8	1.3455	1.3293	1.3383	1.3264	1.1278	1.1123			1.2703	1.2703	1.3455	1.1278
1	1.5054	1.4809	1.4995	1.4758	1.1937	1.1686			1.3996	1.3996	1.5054	1.1937
2	2.4628	2.3899	2.4692		1.6430				2.1989	2.1989	2.4628	1.6430
5	5.7147	5.4999	5.7572		3.4091				4.9969	4.9969	5.7147	3.4091
λ_L (Present)	25.0000				104.8889				32.0000	32.0000	1.5625	6.5556
λ_L (ANSYS)	24.8854				99.0681				30.6653	30.6653	1.5590	6.1989